

Theory of angle-resolved photoemission from the bulk bands of solids. I. Formalism

N. J. Shevchik and D. Liebowitz

Department of Physics, State University of New York, Stony Brook, New York 11794

(Received 7 November 1977)

A theory for describing the angle-resolved photoemission spectra from the bulk bands of solids is developed which views the photoemission process as a single-step coherent emission of electrons from atomic sources into a final state of well-defined momentum. The final state is assumed to be free-electron-like except in the region near the strong atomic potential, where it is distorted into a spherical wave. While the momentum conservation, transport, and escape processes are free-electron-like in nature, the optical ionization process is governed by atomiclike dipole selection rules. The dependence of the peak intensities of the angle-resolved photoemission spectra upon the direction of the polarization of the electric field can be used to determine the orbital composition of the initial states in a very simple manner. The simple form of the theory presented here can be extended to materials having a hybridized final state by the use of a pseudopotential wave function modified by atomic-dipole selection rules. It is argued, however, that the single-unhybridized-final-state wave function is approximately valid for describing the angle-resolved photoemission spectra of all materials, and that the one-dimensional density-of-states model is probably not valid for any material with a lattice constant smaller than the mean free path. An experimental geometry is proposed in which the photoemission intensity is proportional to the charge density of the initial state in the direction of the final-state momentum, similar to the results of previous theories based upon the plane-wave final state.

I. INTRODUCTION

A rigorous description of the angle-resolved photoemission spectra of solids requires a detailed computation of both the initial and final electron states.¹ If one wishes to avoid the computation of the final-state band structure, and still describe the spectra well, it is necessary that the important characteristics of the final states be identified. The pseudo-wave-function of the electronic state inside of the solid having reduced momentum \vec{k} and belonging to band n can be written in terms of a plane-wave expansion²

$$\psi_{n\vec{k}}(\vec{r}) = e^{i\vec{k}\cdot\vec{r}} \sum_{\vec{G}} U_n(\vec{k} + \vec{G}) e^{i\vec{G}\cdot\vec{r}}, \quad (1)$$

where the \vec{G} 's are reciprocal-lattice vectors. In materials having strong pseudopotentials, such as semiconductors, several terms of similar magnitude are contained in the above sum. In materials having a weak pseudopotential, such as metals, only one term in the sum is important for describing the final electron state.

Recent experimental results have shown that the free-electron final state (FEFS) model, in which it is assumed that direct optical transitions take place from the initial states into a single-plane-wave-like final state, serves to locate the peak positions in the angle-resolved photoemission spectra of the noble metals and transition metals.³⁻⁷ However, matrix elements based upon a plane-wave final state do not explain the intensities of the observed peaks.⁶⁻⁸ Wagner *et al.*⁶ found that constant matrix elements explained the

observed intensities better than the plane-wave final state. Furthermore, they recognized that constant matrix elements implied that the final state must consist of several plane waves more or less isotropically distributed, rather than one plane wave.

Earlier work by Janak *et al.*⁹ suggested that constant matrix elements could explain the angle averaged photoemission spectra of Cu. However, Rowe and Smith¹⁰ found that the peak intensities for emission from the (111) and (100) faces of Cu were not explained well by constant matrix elements. If the final state were composed of several plane waves, then more than one final-state band is expected to contribute to the photoemission spectra in any direction, in contradiction to the single band predicted by the plane-wave final-state model, which appears to describe the peak positions well.

A partial resolution of the apparent contradictory behavior of the final state was suggested to be exposed by consideration of an augmented-plane-wave (APW) approximation for the final state.¹¹ In the region inside of the muffin-tin potential, the APW function is expressed as a linear combination of spherical waves, while outside the muffin-tin potential it is expressed as a single plane wave.² The Fourier expansion of the core part of the APW reveals that it has components which are distributed in several directions in k space, thereby allowing more optical transitions to take place than for the simple plane-wave final state. It was suggested that atomiclike dipole selection rules ought to govern the behavior of the photoionization cross section since the atomic potential is

responsible for the finite value of the cross section. However, the region of the wave function external to the core, which is plane-wave-like, ought to govern the momentum conservation, transport, and escape processes. Thus, it was concluded that previous results derived for the plane-wave final state are correct provided that the plane-wave matrix element is replaced with one based upon atomic dipole selection rules.

Although many theories for angle-resolved photoemission have been presented before,¹²⁻¹⁸ we feel that some of them are too complicated to be easily applicable to real systems; the other simplified theories based upon a single plane wave¹⁵ or nearly free final-state models¹² are partly incorrect and incapable of predicting peak intensities realistically. We develop in this paper a theory based upon the free-electron model and atomic dipole selection rules that eliminates the necessity of having to calculate explicitly the final-electron state. The important characteristics of the final state are reduced to a few parameters that can be calculated or fit to experiment. In order to keep the theory simple and transparent so that it can be used by experimentalists to interpret their results, we have deliberately omitted complications and processes that we feel are not important for determining the basic shape of the angle-resolved photoemission spectra. Although we give some argument here for neglecting some effects, the ultimate justification lies in the success of the theory in describing experiment as shown in Paper II. We do not claim our theory to be perfect, but we feel that it provides a simple first-order description for the experimental results.

A preliminary report has already shown that the theory developed here describes the angle-resolved photoemission spectra of Cu very well for $h\nu = 11$ to 40 eV.¹⁹ In Paper II,²⁰ we show that the present theory describes the photoemission spectra from the (111) surface of Ag well, while the plane-wave and constant matrix give generally poor agreement.

The structure of this paper is as follows. In Sec. II, we discuss why a low-energy electron diffraction LEED-type theory is not really necessary to describe photoemission in free-electron-like metals in which the pseudopotential is weak. We also argue that the effects due to the rapid termination of the bulk at the surface are not very important compared to the emission from the bulk bands, particularly for d -band metals.

In Sec. III A, we derive an expression for the photoelectron intensity by considering the photoemission process as a single-step coherent emission of electrons from atomiclike emitters into a free-electron-like final state. In Sec. III B, it is

shown that the assumption of atomic optical selection rules leads to a dipole vector associated with each initial state from which the dependence of the peak intensities for any arbitrary polarization of the electric field and angle of emission can be predicted.

In Sec. IV, it is shown that the model can be used to determine not only the energy bands from the positions of the peaks, but also the orbital composition of the initial states from the dependence of the intensities of the peaks on the direction of polarization of the electric vector.

In Sec. V, it is shown that the theory can be extended to materials in which the crystal potential is strong by employing a pseudopotential calculation.

In Sec. VI, we show that the plane-wave final-state model should be valid for predicting peak positions, not only for metals, but for all materials. It is also shown that simple atomic-dipole-like selection rules become valid at large final-state energies provided that the range of the pseudopotential in k space is finite and the core-like portion of the wave function is unimportant for the transport step.

Finally, in Sec. VII, two experimental geometries are proposed in which only a rotation of the sample is needed to obtain useful information on the electronic charge density and the angular momentum of the initial states.

II. NEGLECT OF SURFACE EFFECTS AND MULTIPLE SCATTERING

In this section, it is argued that the effects of the surface do not make an important contribution to the photoemission spectra of real solids. It is also argued that multiple scattering of final-state electrons can be neglected in noble and probably other metals.

The electromagnetic field produces a perturbation on the electronic states, which can be written as

$$H' = (e/m_e c) \vec{P} \cdot \vec{A} e^{i\omega t}, \quad (2)$$

where \vec{P} is the momentum operator, m_e is the mass of the electron, \vec{A} is the vector potential, and ω is the frequency of the incident light.

The photoionization matrix element of the dipole operator connecting initial state i to final state f is approximately given by²¹

$$M_{fi} \propto \langle \psi_f | \vec{\epsilon} \cdot \nabla V(\vec{r}) | \psi_i \rangle, \quad (3)$$

where $V(\vec{r})$ is the total one-electron potential and $\vec{\epsilon}$ is the direction of the electric vector inside of the solid. As pointed out by Feibelman,²² this form for the matrix element is not rigorously cor-

rect since the effective one-electron potential is in general energy dependent. However, for the present discussion, the above matrix element is suitable. Although the abrupt change of the potential at the surface gives an important contribution to the photoionization matrix element in the free-electron model,¹² where contributions from the bulk is zero, its contribution in real materials should be insignificant compared to the emission from the bulk. The strength of the potential gradient at the surface is at most on the order of

$$\bar{\nabla}V(r)|_s \approx W/a, \quad (4)$$

where W is the inner potential, which is on the order of 14 eV, and a is the interatomic spacing. This gradient is considerably smaller than the gradient in the vicinity of the cores of atoms near the surface. As the wavelength of the final state becomes less than a (corresponding to $h\nu > 10$ eV), the photoionization cross section of the surface potential region should become much less than that arising from the regions of the initial-state wave functions in the vicinity of the atomic cores.

Presently, we are neglecting the possibility that the vector potential inside of the solid can change very rapidly at the surface²²⁻²⁴ and take it to be a constant. However, as we show in Paper II, this assumption yields reasonable results.

It has been suggested that a formalism such as that developed for low-energy electron diffraction, which takes into account multiple scattering of the final state, is needed to describe the angle-resolved photoemission spectra of even the noble metals.^{18,25} A LEED-type formalism is needed to describe LEED, since deviations of the electronic states away from free-electron-like behavior produce the diffraction patterns of interest. However, in photoemission the deviations of the final state away from the free-electron behavior in many metals carries a very small part of the photocurrent. The neglect of these deviations by the use of a single APW-like final state in photoemission should not be serious. In materials where the crystal potential is large, a pseudopotential calculation²⁶ should suffice to account for the multiple scattering in the bulk. However, as we shall discuss in Sec. VI, the dipole matrix elements from such a wave function must be modified to yield correct results.

III. COMPUTATION OF THE ANGLE-RESOLVED PHOTOEMISSION SPECTRA

In Sec. IIIA, we review the formulation of the photoemission spectra for the simple plane-wave final state and in Sec. IIIB, we derive the angular dependence of the atomic cross sections that are

to replace those calculated for the plane-wave final state.

A. Plane-wave final-state model

In this section, we begin the development of the theory by considering the photoemission process not in terms of the three-step model,²⁷ but as a single-step coherent emission of atomic sources of electrons into a plane-wave-like final state modified to take into account the strong core potential of the atoms.

We assume that the initial state for a solid with one atom per unit cell can be written in the tight-binding approximation as

$$\psi_{\mathbf{k}_i n}(\mathbf{r}) = \sum_{j, m, l} e^{i\mathbf{R}_j \cdot \mathbf{k}_i} C_{im}^n(\mathbf{k}_i) \phi_{im}(\mathbf{r} - \mathbf{R}_j), \quad (5)$$

where \mathbf{R}_j is a lattice site, $\phi_{im}(\mathbf{r})$ is an atomic orbital of angular momentum l and projection m , and the $C_{im}^n(\mathbf{k}_i)$'s are the coefficients of the respective orbitals describing the band n . We also assume that the tight-binding wave function remains valid right up to the last layer of atoms on the surface, where the potential abruptly increases by the amount W . The portion of the wave function extending into the vacuum can be expanded in terms of decaying plane waves, but, as discussed in Sec. II, it does not usually make an important contribution to the photoemission spectrum of real solids, and is therefore neglected here.

We assume for now that the final state inside of the solid is a single plane wave with momentum \mathbf{k}_f . Continuity of the wave function at the surface requires that the parallel components of the momentum of the photoelectron inside and outside of the surface be equal. The energy dispersion of the electron in the vacuum outside of the solid with momentum \mathbf{k}'_f is given by

$$E = \hbar^2 (k'_f)^2 / 2m_e, \quad (6)$$

where m_e is exactly the free-electron mass. The component of momentum perpendicular to the surface inside the solid is given by

$$k_{f\perp} = (k_f^2 - k_{\parallel}^2)^{1/2}, \quad (7)$$

where k_f is the magnitude of the momentum inside of the solid, given by

$$\hbar^2 k_f^2 / 2m_e^* = E + W \equiv E_f(\mathbf{k}_f). \quad (8)$$

The right-hand side of Eq. (8) ought to be the energy of the electron with respect to the lowest s -like band.⁶ The effective mass m_e^* is not necessarily equal to the free-electron value, but takes into account residual lattice interactions and correlation effects.¹⁰ We also neglect the fact that the surface potential mixes together the plane

waves propagating to and away from the surface. The justification for this is in the Appendix.

It can be shown by using a free-electron Green's function that the amplitude of the wave function of a tight-binding electron photoemitted into a plane-wave final state at a distance far from the surface is given by^{12,15}

$$\psi \sim \sum_m M_n(\vec{k}_f, \vec{\epsilon}) e^{i\Delta\vec{k}\cdot\vec{R}_m} \exp(-Z_m/2\lambda \cos\theta), \quad (9)$$

where $M_n(\vec{k}_f, \vec{\epsilon})$ is photoionization matrix element of the atom orbital corresponding to band n , Z_m is distance of atom m from the surface, and $\Delta\vec{k} = \vec{k}_f - \vec{k}_i$. (The same expression arises when we consider the atoms to be coherent emitters of electrons in a manner similar to the antenna problems given in freshman physics courses.) The quantity λ is the mean free path of the photoelectron and θ is the angle that \vec{k}_f makes with respect to the surface normal. The exponential term in Eq. (9) expresses the reduced contributions to the coherent photoelectron current from atoms that lie deeper into the solid.^{15,16} Such a reduction is brought by the inelastic scattering of the photoelectron with the valence electrons and plasmons. The inelastically scattered electrons produce a structureless background to the emission spectra which shall be neglected here.

An additional contribution to the effective mean free path occurs when there exists at certain energies no states in the bulk of the proper symmetry that can couple to the external plane-wave state.¹⁶ In this case the external wave decays into the bulk via Bragg reflection forces. Since the inelastic damping of the electron is large, this contribution to the effective mean free path might not ever be large enough to cause a noticeable weakening of k conservation, but it might cause a noticeable modulation in the heights of various peaks in the spectra.

Performing the sum over the lattice sites and including energy conservation, we find that the photoelectron emission current can be written

$$I(E_f(\vec{k}_f), \vec{\epsilon}) \propto \sum_n \int M_n(\vec{k}, \vec{\epsilon})^2 [\Gamma^2 + (k_{f\parallel} - k_{i\parallel})^2]^{-1} \times \delta(E_f(\vec{k}_f) - E_n(\vec{k}) - \hbar\omega) d\vec{k}_\perp, \quad (10)$$

where

$$\Gamma = 1/\lambda(\vec{k}_f) \cos\theta, \quad (11)$$

and

$$\vec{k} = \vec{k}_{f\parallel} + \vec{k}_\perp. \quad (12)$$

The Lorentzian factor in Eq. (10) accounts for the

relaxation of the component of the momentum perpendicular to the surface due to the inelastic processes which give rise to a finite mean free path. The summation index n extends over the filled electron bands. We point out that the extended momentum is used in the expressions in Eq. (10). The $E_f(\vec{k})$ as given by Eq. (8) is not periodic in \vec{k} , while the $E_n(\vec{k})$ of the tight-binding initial state is periodic in \vec{k} .

For a plane-wave final state, it has been shown that the photoionization cross section of an atomic orbital, $\phi_n(\vec{r})$, has the form¹⁵

$$|M_n(\vec{k}, \vec{\epsilon})|^2 = |\vec{k} \cdot \vec{\epsilon}|^2 \left| \int \phi_n(r) e^{i\vec{k}\cdot\vec{r}} d^3r \right|^2. \quad (13)$$

The cross section vanishes whenever the component of the vector potential or the electronic charge density of the initial state in the direction of the final-state momentum is zero. The angular dependence of the atomic matrix element is the primary weakness of the plane wave model^{8,9} and we now suggest a matrix element which yields results in far better agreement with experiment.

B. Atomiclike photoionization cross sections

In order to calculate the angular dependence of the matrix element $M_n(\vec{k}, \vec{\epsilon})$, we need to make only two assumptions: (i) Atomic dipole selection rules $\Delta m = 0, \pm 1$ are obeyed.²⁸ (ii) The true final state can be accurately expanded about an atomic site in terms of spherical waves having $m = 0$ only about its direction of propagation.^{8,11} The first assumption is plausible since the portion of the initial and final state in the vicinity of the atomic cores makes the dominant contribution to the photoionization cross section, particularly as the photon energy increases.²⁹ The second assumption can be seen to be reasonable since this fact is true for augmented, orthogonalized, and simple plane waves.² Implicit in this assumption is that the crystal pseudopotential is weak or there is little multiple scattering.

The calculation of the matrix elements based upon the above considerations is facilitated by the use of the coordinate system in which the z axis is taken to lie along the direction of \vec{k}_f and the x and y axes are taken to be perpendicular to the z axis. Application of the atomic selection rules indicates that the following initial-state atomic orbitals can be photoexcited into the final state satisfying assumption 2 by the corresponding vector-potential components.

Vector potential Atomic orbital

$$\begin{array}{ll} A_x & p_x, d_{xz} \\ A_y & p_y, d_{yz} \\ A_z & s, p_z, d_{z^2} \end{array}$$

The x and y components of the vector potential excite initial states having $|m|=1$, while the z vector potential excites states for which $m=0$. The optical transition probabilities for the two $m=1$ states might differ from those of the $m=0$ states. We suggest that the ratios of the $m=0$ to $m=1$ matrix elements computed for isolated atoms²⁸

$$\xi_l \equiv \frac{M_{l,m=0}}{M_{l,m=1}} = \begin{cases} \sqrt{2} \left(\frac{l}{l+1} \right)^{1/2} & \text{for } l \rightarrow l-1 \\ -\sqrt{2} \left(\frac{l+1}{l} \right)^{1/2} & \text{for } l \rightarrow l+1 \end{cases} \quad (14)$$

are approximately valid in the solid. At lower photon energies the formula for the $l \rightarrow l-1$ channel is valid, but at higher photon energies the $l \rightarrow l+1$ channel becomes important.

The above considerations suggest that the angular dependence of the photoionization matrix elements can be more conveniently expressed as

$$|M_n(\vec{k}, \vec{\epsilon})|^2 = |\vec{\epsilon} \cdot \vec{P}_n(\vec{k})|^2, \quad (15)$$

where $\vec{P}_n(\vec{k})$ is a dipole vector associated with the atomic orbital associated with initial state n , which can be written as a sum of vectors for each angular-momentum shell

$$\vec{P}_n(\vec{k}) = \sum_l \vec{P}_l^n(\vec{k}). \quad (16)$$

The components of the above sum in terms of the initial state orbitals are

$$\begin{aligned} \vec{P}_d^n(\vec{k}) &= \bar{M}_d(|k|) [C_x^n(\vec{k})\hat{x} + C_y^n(\vec{k})\hat{y} + \xi_d C_z^n(\vec{k})\hat{z}], \\ \vec{P}_p^n(\vec{k}) &= \bar{M}_p(|k|) [C_x^n(\vec{k})\hat{x} + C_y^n(\vec{k})\hat{y} + \xi_p C_z^n(\vec{k})\hat{z}], \\ \vec{P}_s^n(\vec{k}) &= \bar{M}_s(|k|) C_s^n(\vec{k})\hat{z}, \end{aligned} \quad (17)$$

where the $\bar{M}(\vec{k})$'s are the photoionization amplitude obtained for a pure $m=1$ initial state. The $\bar{M}(|\vec{k}|)$'s, which do not depend upon the angle of emission, but only upon the magnitude of \vec{k} , account for the photon energy dependence of the photoionization cross section. The $\bar{M}(\vec{k})$'s calculated for the free atom²⁹ ought to describe the matrix elements for the solid reasonably well. The $C_{lm}^n(k_i)$'s, the coefficients of the atomic orbitals used to express the initial state (see Eq. 5), are defined with respect to the coordinate system described above and are assumed to be periodic in k -space. However, the $P^n(k)$'s are not periodic in \vec{k} space since the $M(|\vec{k}|)$'s and ξ_i 's depend upon the magnitude of $|\vec{k}|$.

If one is interested in only the dependence of the shapes of the peaks upon the angle of emission for a fixed photon energy, it is not necessary to calculate the $M(k)$'s. In this case, only the parameter ξ_i is needed to characterize the contribution of the final state to the atomic photoionization cross section.

At first glance, the present theory might appear to be schizophrenic. On one hand we use a plane-wave final state to derive Eq. (10), then we throw out the plane-wave atomic cross section and replace it with one based upon atomic-dipole selection rules. Our justification for doing this comes from consideration of an APW, which serves as an approximate final-state wave function.⁹ The energy conserving δ function in Eq. (10) arises independently of the spatial behavior of the final-state wave function and does not need to be considered. The Lorentzian factor in Eq. (10) depends upon the variation in the phase of the final state from one atomic site to another. This phase variation, which depends primarily upon the behavior of the final state between the atomic cores, should be approximated adequately by a plane wave. The mean free path of the electron is primarily a "jellium" effect, for which a plane wave is also adequate. However, the dominant contribution to the photoionization does not come from the region between the atoms where the final state is free-electron-like, but rather from the region near the atomic cores, where it is distorted into a spherical wave.

As discussed previously,¹¹ the distortion of the true final state into a spherical wave in the vicinity of the atomic core implies that its Fourier transform in k space is not a single plane wave, but has additional components, which can produce secondary-emission cones. While these additional components make the primary contribution to the photoionization cross section, their total contribution to the secondary cones is estimated using Eq. (54) in Ref. 11 to be $\sim 10\%$ for the photon energies of ~ 20 eV.

IV. IMPLICATIONS OF THE MODEL

The important features of the model derived in Secs. I-IV are (a) that only a single region in the initial-state Brillouin zone contributes to the spectra in any given direction and (b) that the polarization dependence of the initial state is that of a single complex dipole vector which is expressible in terms of the orbitals of the initial state. When this model is valid, the first feature allows the electron energy bands to be determined from the positions of the peaks in the observed spectra from a single crystallographic surface. Now we

shall demonstrate that feature (b) allows the wave functions to be determined from the dependence of the amplitude of the observed peaks upon the direction of polarization.

A. Initial-state orbitals

In the case where the $C_{im}^n(k)$'s are real (e.g., in solids having inversion symmetry and a small spin-orbit interaction) the intensity vanishes when the electric vector is perpendicular to \vec{P}_n , and it is maximum when it is parallel to \vec{P}_n . (This is in contrast to the predictions of the plane-wave final state where the maximum intensity occurs for all initial states when the electric vector is parallel to the direction of emission.) From inspection of Eq. (17), it is clear that the coefficients of three components of the wave function can be identified when the direction of \vec{P}_n is found.

When the coefficients in the initial-state wave function are complex (e.g., in systems lacking inversion symmetry or having a large spin-orbit interaction), the polarization vector is complex, consisting of a real vector and an imaginary vector. Maximization of the intensity by altering the direction of the vector potential will not yield the direction of both components of \vec{P}_n ; it might be necessary to plot out a more detailed dependence of the behavior of the intensity to find the two components.

In practice, it is cumbersome to change the orientation of the electric field to maximize the intensity of the peak of interest in order to find \vec{P}_n . A less difficult method is clearly desirable. We note that the derivative of the intensity with respect to the direction of the electric field is

$$dI \propto d\vec{\epsilon} \cdot \vec{P}_n (\vec{\epsilon} \cdot \vec{P}_n). \quad (18)$$

From the above equation we see that by measuring the change in the intensity for three small independent displacements of $\vec{\epsilon}$, \vec{P}_n can be found. When the polarization vector is complex, the change in intensity is

$$dI \propto d\vec{\epsilon} \cdot [\text{Re}(\vec{P}_n) + \text{Im}(\vec{P}_n)] (\vec{\epsilon} \cdot \vec{P}_n). \quad (19)$$

In order to find the two components of \vec{P}_n , the above procedure must be applied for two different $\vec{\epsilon}$'s.

Equations (15)–(17) imply that in general the orientation and magnitude of the polarization vector of any initial state depends upon the angle of emission since the orientation of the coordinate system in which the $C_{im}^n(k)$'s are defined changes with this angle. If we were to observe the initial state from some other direction, the polarization vector would be different. For *s*-like initial states, the polarization vector is always along

the axis of emission. For initial states consisting entirely of *p* orbitals, it is sufficient to observe the polarization vector for only one direction of emission to determine the orbital composition of the initial state. We note that in the case where $\xi = 1$, the three polarization vectors of the *p* states are orthogonal and their orientation remains independent of the direction of emission. When the emission is maximized for one pure *p*-like state, the emission for the other two vanishes.

Since the orbitals for which $|m| = 2$ with respect to the axis of emission cannot contribute to the spectra for any polarization direction, the polarization vector of the *d* states must always depend upon the direction of emission. Such $m = 2$ orbitals can contribute to the spectra in other directions of emission, since with respect to other axes, they are not purely $|m| = 2$ orbitals. In order to obtain the complete set of the 5*d* orbitals composing a state, it is necessary to find the polarization vectors for two different directions of emission.

B. Photon energy dependence

The value of the parameter ξ_l depends upon the relative strengths of the $l \rightarrow l+1$ and $l \rightarrow l-1$ optical transition channels, which is expected to vary with photon energy. For now let us ignore the variations in this parameter with photon energy.

When the initial state consists of orbitals from the same angular momentum shell, we expect the direction of the polarization vector for a constant direction of emission to remain independent of the photon energy; however, when the initial state consists of orbitals with different angular momenta, the direction of the polarization vector is altered since the magnitude of M_l 's changes with the photon energy. In fact the variations in the M_l 's with $h\nu$ can, in principle, be used to obtain the complete orbital, both *l* and *m*, compositions of the initial state.

The orientation of the initial state orbitals is largely determined by \vec{k}_i , thus for a fixed polarization direction, the relative strengths of the peaks in the angle-resolved photoemission spectra depends upon the angle between \vec{k}_i and \vec{k}_f . For emission along a crystallographic axis, \vec{k}_i and \vec{k}_f are parallel for all photon energies. In this case, we expect the shape of the spectra to be a periodic function of \vec{k}_f . However, for a finite $k_{||}$, the angle between \vec{k}_i and \vec{k}_f is given by

$$\cos \theta_{if} = \frac{k_{i||}k_{f||} + k_{i\perp}k_{f\perp}}{|k_{i||}^2 + k_{i\perp}^2|^{1/2}|k_{f||}^2 + k_{f\perp}^2|^{1/2}}. \quad (20)$$

In the above expression \vec{k}_i is taken to be the reduced momentum and \vec{k}_f is taken to be the extend-

ed momentum. As the photon energy increases and $k_{f\perp} \gg k_{f\parallel}$, the asymptotic behavior of the angle between \vec{k}_i and \vec{k}_f , θ_{if} is given by

$$\cos \theta_{if} = \frac{k_{i\perp}}{(k_{i\parallel}^2 + k_{i\perp}^2)^{1/2}}. \quad (21)$$

The largest variations in the shapes of the spectra with photon energy for a fixed k_{\parallel} are expected to occur when the changes in θ_{if} are the greatest. The changes in θ_{if} become larger as $k_{i\parallel}$ increases. Variations in the shape of the spectra with photon energy should be particularly large for d -like initial states. For emission along a crystallographic axis, initial states having $|m| = 2$ should not be seen for any photon energy, provided that the final state remains unhybridized. However, the $|m| = 2$ initial states should become visible when the angle between \vec{k}_i and \vec{k}_f increases. This should happen for non-normal emission from initial states closest to the Γ point.

The observed variations with photon energy of the peak intensities in the angle-averaged photoemission spectra of noble metals³⁰ might be explained by variations in the average angle between \vec{k}_i and \vec{k}_f . When several reciprocal-lattice vectors lie close on a sphere of radius k_f , large areas exist where \vec{k}_i and \vec{k}_f are nearly perpendicular. In this case, emission from orbitals which have an $|m| = 2$ with respect to \vec{k}_i should become more intense. Most of the $m = 2$ orbital components are at lower initial state energies. As \vec{k}_f increases or decreases, \vec{k}_i is less often perpendicular to \vec{k}_f and contributions from such $m = 2$ states become less intense.

Angle-averaged photoemission spectra taken in the $h\nu \sim 11$ –40 eV regions usually show that the strength of the more tightly bound electrons increases with the photon energy.³¹ For low photon energies ($h\nu < 20$ eV) where optical transitions take place to states in the second Brillouin zone in the extended zone scheme, \vec{k}_i and \vec{k}_f are nearly parallel to one another in all directions. Thus emission from the $m = 2$ initial states should be weak even in the angle-averaged photoemission spectra. As the photon energy increases, the emission from the $m = 2$ states ought to increase as the average angle between \vec{k}_i and \vec{k}_f increases.¹

According to our model, optical transitions occur into all free-electron bands with similar probabilities. Since each free-electron band propagates in different directions, we expect the angle-averaged spectra to reveal eventually, as the photon energy is increased, the total electron density of initial states derived from orbitals in the same shell, provided that the effects of charge-density overlap between adjacent orbitals is taken into account.³² The conditions for the onset of density-

of-states behavior given by Feibelman and Eastman¹⁶ are correct. However, the angle-resolved spectra should still reveal only a single point in \vec{k} space, provided that the effects of thermal displacements does not eliminate k conservation.¹⁰ The angle-resolved photoemission spectra are unlikely to ever reflect one-dimensional density of states as discussed below.

We also note that the atomic-dipole matrix elements, the plane-wave, and constant matrix elements should yield similar angular averages as the photon energy increases. However, their differences clearly show up in the angle-resolved photoemission spectra taken at low photon energies.²⁰

V. EXTENSION TO STRONGLY HYBRIDIZED FINAL STATES

In this section, we suggest how the theory developed in Secs. I–IV can be extended to the case in which the final state wave function consists of a strong admixture of hybridized waves. As discussed by Smith *et al.*³³ the photoemission intensity from a tight-binding initial state into a plane wave component of momentum \vec{k}_f of a Bloch-like final state is given by

$$|M_{if}|^2 \propto |U_n(\vec{k}_f)|^2 \left| \sum_{\vec{G}} \vec{\Lambda} \cdot \vec{G} U_n(\vec{k}_i + \vec{G}) \tilde{\psi}^*(\vec{k}_i + \vec{G}) \right|^2, \quad (22)$$

where $\tilde{\psi}(\vec{k})$ is the Fourier transform of the initial-state orbital. Since it has been shown that a single plane wave yields the incorrect angular dependence for the photoionization cross sections,^{7–9} we expect cross sections computed from a pseudopotential wave function, which is a sum of plane waves, to yield incorrect results also. Since the coefficients $U_n(\vec{G})$ obtained from a pseudopotential calculation should yield essentially the same coefficients as for an APW-like calculation, Eq. (22) can be corrected by introducing the polarization vector corresponding to the direction of every plane wave component:

$$|M_{if}|^2 \propto |U_n(\vec{k}_f)|^2 \left| \vec{\epsilon} \cdot \sum_{\vec{G}} \vec{P}^*(\vec{k}_i + \vec{G}) U_n(\vec{k}_i + \vec{G}) \right|^2. \quad (23)$$

For this case, the complicated final state makes it difficult to extract information concerning the orbital composition of the initial state.

VI. VALIDITY OF THE SINGLE-WAVE FINAL STATE

In this section, we investigate the conditions under which the simple "free-electron" model de-

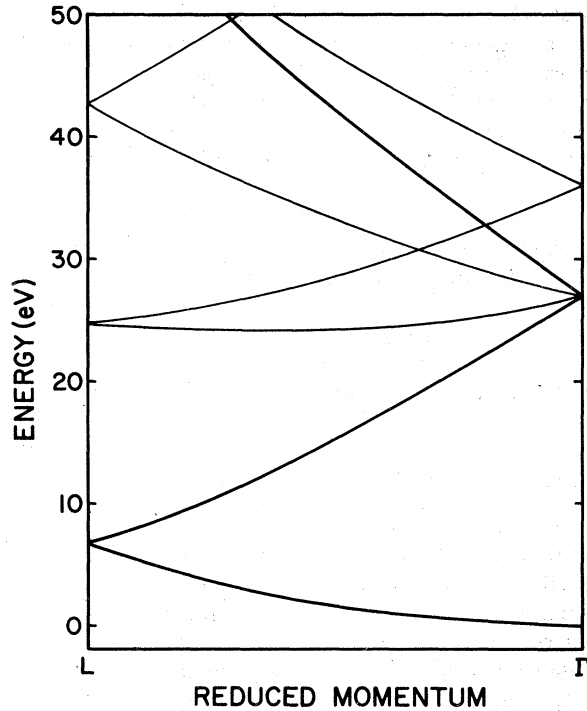


FIG. 1. Free-electron band structure along the [111] axis of the face-centered-cubic structure.

veloped in Secs. I–V is valid. In order to do this, let us consider the free-electron band structure along the [111] axis of the fcc lattice as is shown in Fig. 1.² The heavy line indicates the energy dispersion of the plane wave having a momentum directed along the [111] axis; the extended momenta of the other bands are pointing in some other directions. Since this solid band is the only one that can be matched at the surface to an external plane wave propagating normally to the surface, the amount of admixture of this band determines the probability that a photoexcited electron can get out of the solid in a direction normal to the surface. According to the model outlined in Sec. III, electrons are photoexcited into all final-state bands with nearly equal probabilities, and thus the contributions to the spectra in any given direction are governed largely by the transport and escape processes.

According to first-order perturbation theory, the amount of admixture between two plane waves having the same reduced momentum is²

$$V_{12}(\Delta\vec{k})/\Delta E_{12}(k), \quad (24)$$

where ΔE_{12} is the energy separation between the two states, $V_{12}(\Delta\vec{k})$ is pseudopotential interaction between them, and $\Delta\vec{k}$ is the difference in the extended momentum of the two waves. In order for two bands to mix appreciably, their energy sep-

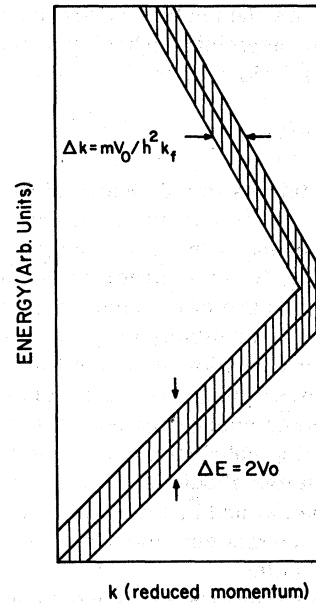


FIG. 2. Free-electron band propagating normal to the surface in the high-energy limit where the density of all bands becomes continuous. The shaded region shows where the free-electron state becomes distributed in the $E-k$ plane.

aration must be no more than the pseudopotential interaction. Since typical pseudopotential interactions are on the order of 5 eV,²⁶ inspection of Fig. 1 shows that there are large regions of the Brillouin zone where the admixture of the solid band is very weak. For example, the band at 25 eV near the L point is separated by ~ 15 eV from the solid bands and therefore it makes much smaller contribution to the spectra than the solid band near the Γ point at the same energy.

Now let us consider the bands at much higher energy where the density of the bands becomes nearly continuous. When the pseudopotential is constant, independent of the momentum difference, the free-electron band n of momentum \vec{k}_f becomes distributed vertically in energy according to

$$|U_{k_f}(E)|^2 = (1/\pi)\{V_0/[E - E_n(\vec{k}_f)]^2 + V_0^2\}. \quad (25)$$

It is obvious that a vertical broadening of the solid band leads to a corresponding horizontal broadening in k space as is illustrated in Fig. 2. Using Eqs. (8) and (25), we find that for a fixed final-state energy this plane wave is distributed horizontally in k space as

$$|U(\vec{k})|^2 = (1/\pi)[\beta/(\vec{k} - \vec{k}_f)^2 + \beta^2], \quad (26)$$

where

$$\beta = mV_0/\hbar^2 k_f. \quad (27)$$

The above result shows that the free-electron band is distributed over a range 2β in \vec{k} space, but peaks at the free-electron momentum. For typical semiconducting materials, we find that the free-electron band is distributed only over about one fourth of the Brillouin zone for final-state energies of about 20 eV above the Fermi level. As the final-state photon energy increases, ξ decreases even further. According to these estimates the one-dimensional density-of-states model³⁴⁻³⁶ cannot be justified by hybridization of the final-state bands alone; a very strong relaxation of the component of momentum perpendicular to the surface is needed to justify this model. (However, as discussed earlier,⁹ the plane wave components arising from the core part of the final states might become sufficiently important at high energies to make the one-dimensional density-of-states model valid.) We conclude that the single-plane-wave final state, according to the present calculations, should be at least qualitatively valid for locating the region in the Brillouin zone contributing to the angle-resolved photoemission spectra for nearly all materials and photon energies. This is fortunate since many of the complications due to surface irregularities might not ever be important.⁹

Although the plane-wave final state serves to locate the points in k space contributing to the spectra even when the pseudopotential has infinite range in k space, the matrix elements derived for a single-plane-wave final state in Sec. III might not necessarily be valid. If the range of the pseudopotential in k space is G' , then plane waves having propagation directions separated by at most the angle

$$\Upsilon \cong \tan^{-1}(G'/k_f) \quad (28)$$

are mixed appreciably. In order for the matrix elements for a single plane wave to be valid, it is necessary that Υ be small. When Υ is large, the contributions from all of the plane-wave components should lead to matrix elements that are nearly constants, but which still obey crystal dipole selection rules. Evidence has already been presented for Ag which indicates that the simple unhybridized wave final state is not adequate at $h\nu \sim 40$ eV and that constant matrix elements work better.⁸ Thus we conclude that the simple model presented here becomes more valid as the final-state energy increases.

The above analysis is valid in the limit that the density of bands is large; at lower photon energies ($h\nu < 20$ eV) in noble metals, the number of bands available for hybridization is small, and thus a single-plane-wave-like final state ought

to be valid. Indeed, experimental results show this to be the case.^{8,19,20}

VII. EXPERIMENTAL ARRANGEMENTS

In order to exploit the polarization dependence fully, it is convenient to have a light source which is fixed but for which the polarization vector can be rotated to any angle with respect to the Poynting vector. In the experimental arrangement shown in Fig. 3, the analyzer and the sample can be rotated in the plane defined by the directions of the detected electron and of the incident light. This arrangement allows the polarization direction with respect to the sample to be varied in every direction by a combination of a rotation of $\vec{\epsilon}$ about the Poynting vector and a rotation of the sample. In order to keep the angle of emission constant while changing $\vec{\epsilon}$, it is necessary to move the analyzer. One difficulty with this method might arise when the refraction of the light at the surface alters the polarization direction and phase inside the solid.

In practice, it might be cumbersome to find the atomic polarization vectors \vec{P}_n , since a two-parameter space has to be scanned as discussed in Sec. IV. However, two geometries exist which

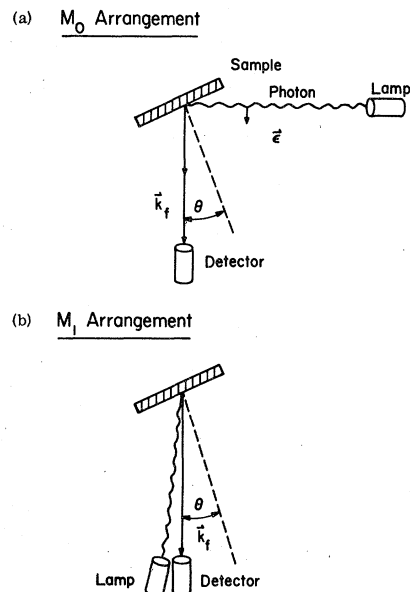


FIG. 3. (a) M_0 experimental arrangement for which only initial states having orbital angular momentum projection $m=0$ with respect to the final-state momentum \vec{k}_f can make a contribution to the photoemission spectra. The $m=0$ component of the initial-state band structure is obtained by scanning θ , the angle between \vec{k}_f and the normal to the sample via a rotation of the sample. (b) M_1 experimental arrangement for which only initial states having $m=1$ can contribute to the spectra.

yield useful results without much effort.

When the light source and the analyzer are at 90° with respect to one another and $\vec{\epsilon}$ is directed toward the analyzer, as shown in Fig. 3(a), only the $m=0$ initial states can contribute [see Eq. (16)]. Such spectra give an indication of the amount of charge density of the initial state is directed toward the analyzer, similar to the predictions of the plane-wave final-state model.¹⁵ A simple rotation of the sample, holding the analyzer and light source fixed, then yields the $m=0$ orbital projection of the initial-state band structure.

When the angle between the analyzer and the light source lie along nearly the same line, as in Fig. 3(b), the spectra yield a $m=1$ projection of the band structure. For this configuration, an unpolarized light source yields the total $m=1$ projection.

VIII. SUMMARY AND CONCLUSIONS

We have presented a model for describing the angle-resolved photoelectron spectra of solids, which we believe takes into account the important physical processes. The following are the relevant characteristics of our model. (i) The photoemission process is viewed as a single-step coherent emission of electrons from atomic sources. (ii) The final state is an unhybridized wave containing spherical waves with only $m=0$ angular momentum projections with respect to the direction of \vec{k}_f . (iii) Atomiclike dipole selection rules govern the behavior of the cross sections of the atoms so that only initial states having $m=0, \pm 1$ values can be photoexcited. (iv) The transport momentum conservation and escape processes are free-electron-like in nature. The conservation of the component of momentum perpendicular to the surface is partially relaxed by the inelastic scattering processes. (v) Optical transitions take place into all bands with similar probabilities, but the transport and escape probabilities differ significantly for each band and thus they largely determine the contributions to the spectra in any direction. (vi) The contributions to the spectra from the surface potential are unimportant.

The dependence of the intensities of the peaks upon the angle of emission and polarization direction of the photon field is significantly different from that predicted by either a plane wave or constant matrix elements, as will be demonstrated in detail in Paper II. The model is sufficiently simple so that it can be used to extract from experimental data information on the energy bands and the eigenvectors of the filled electronic states. In particular, the model introduced here shows

that the application of polarized light can open up another dimension of usefulness for angle-resolved photoemission.

The simple form of the model presented in Sec. III is expected to be approximately valid at the onset of photoemission for most metals in which the pseudopotential is weak, but it should become valid for materials in which the pseudopotential is strong as the photon energy increases. For such materials at lower photon energies the pseudopotential method can be used to describe the final state of the photoelectron, provided that the cross sections are modified according to the prescription given in Sec. IV.

The present theory still needs to be tested with polarized light sources and to photon energies extending above 40 eV. Due to difficulties in performing high-resolution angle-resolved experiments in the x-ray regime, it might be necessary to compare the predictions of this model with more sophisticated band calculations that take into account the potential of the atomic cores.

ACKNOWLEDGMENTS

Discussions with P. B. Allen, W. H. Butler, J. Colbert, B. Gyorffy, J. Lawrence, F. Pinsky, M. Sagurton, and J. W. Serene are gratefully acknowledged. This work was supported in part by the NSF under Grant No. DMR-76-12574.

APPENDIX: MIXING OF THE PLANE WAVES AT THE SURFACE

In the photoemission experiment, the wave function outside of the solid is a single plane wave propagating away from the surface with a wave vector \vec{k}' . In order for the wave function and its derivative outside of the solid to be continuous at the surface, in which the potential jumps abruptly, the wave function inside of the surface must have the form

$$\psi_i(r) = \frac{e^{i\vec{k}_i \cdot \vec{r}}}{2} \left[\left(1 + \frac{k'_1}{k_1}\right) e^{+ik_1 z} + \left(1 - \frac{k'_1}{k_1}\right) e^{-ik_1 z} \right], \quad (\text{A1})$$

where the unprimed k 's correspond to the momentum components inside of the solid. The first term in brackets corresponds to a plane wave propagating towards the surface, while the second corresponds to one propagating away from the surface. In the development of the theory in Sec. III, we have assumed that only the plane wave propagating towards the surface makes an appreciable contribution to the spectra. For free electrons, we find that

$$\frac{k'_1}{k_1} = \left(\frac{mE \cos^2 \theta_e}{m^*(E+W) - mE \sin^2 \theta_e} \right)^{1/2}, \quad (\text{A2})$$

where θ_0 is the angle between \vec{k}' and the normal to the surface. The above two expressions indicate that large contributions to the emission spectra should come from the plane wave propagating away from the surface, particularly in the ultraviolet photoemission regime at large emission angles. However, as we shall show in Paper II,²⁰ there is little evidence for such contributions.

We believe that the contributions to the spectra from the state propagating away from the surface is reduced because the true potential does not jump abruptly, but rises to the vacuum potential over a distance of an interatomic spacing. For a one-dimensional step potential, the Born approximation for the reflection coefficient of an incident plane wave is³⁷

$$R = \frac{m^2}{(\hbar k)^2} \left| \int_{-\infty}^{\infty} e^{-2ikz} U(z) dz \right|^2. \quad (\text{A3})$$

An integration by parts yields

$$R \cong \frac{m^2}{4(\hbar k)^4} \left| \int_{-\infty}^{\infty} \frac{dU(z)}{dz} e^{-2ikz} dz \right|^2. \quad (\text{A4})$$

For the potential step of amount W , Eq. (A4) yields

$$R = [m^2/4(\hbar k)^2] |W|^2 \quad (\text{A5})$$

which is equal to the leading term in a power-series expansion in W of the exact result for the reflection coefficient. When the potential rises over a distance σ so that

$$\frac{dV(z)}{dz} \propto e^{-z^2/2\sigma^2}, \quad (\text{A6})$$

then Eq. (A4) yields

$$R = [m^2/4(\hbar k)^2] |W|^2 e^{-\sigma^2 k^2}. \quad (\text{A7})$$

The above expression shows that Eq. (A1) is valid when the wavelength of the electron is longer than σ ; however, when the wavelength of the electron is comparable to σ , the contribution from the wave propagating away from the surface is far less important than for the abruptly rising potential. Since σ is on the order of an interatomic spacing, we expect the R to be small when $h\nu \sim 20$ eV.

¹W. D. Grobman, D. E. Eastman, and J. L. Freeouf, Phys. Rev. B **12**, 4405 (1975).

²J. Callaway, *Energy Band Theory* (Academic, New York, 1964).

³P. M. Williams, P. Butcher, J. Wood, and K. Jacobi, Phys. Rev. B **14**, 3215 (1976).

⁴R. J. Baird, L. F. Wagner, and C. S. Fadley, Phys. Rev. Lett. **37**, 111 (1976).

⁵J. Stöhr, P. S. Wehner, R. S. Williams, G. Apai, and D. A. Shirley (unpublished).

⁶L. F. Wagner, Z. Hussain, and C. S. Fadley, Solid State Commun. **21**, 257 (1977).

⁷D. Liebowitz and N. J. Shevchik, Phys. Rev. B **17**, 3825 (1978).

⁸N. J. Shevchik and D. Liebowitz, Phys. Rev. B **16**, 2395 (1977).

⁹J. F. Janak, A. R. Williams, and V. L. Moruzzi, Phys. Rev. B **11**, 1522 (1975).

¹⁰J. E. Rowe and N. V. Smith, Phys. Rev. B **10**, 3207 (1974).

¹¹N. J. Shevchik, Phys. Rev. B **16**, 3428 (1977).

¹²G. D. Mahan, Phys. Rev. B **2**, 4334 (1970).

¹³W. L. Schaich and N. W. Ashcroft, Phys. Rev. B **3**, 2452 (1971).

¹⁴C. Caroli, D. Leder-Rosenblatt, B. Roulet, D. Saint James, Phys. Rev. B **8**, 4552 (1973).

¹⁵J. W. Gadzuk, Phys. Rev. B **10**, 5030 (1974), and in *Electronic Structure and Reactivity of Metal Surfaces* (Plenum, New York, 1976).

¹⁶P. J. Feibelman and D. E. Eastman, Phys. Rev. B **10**, 4932 (1974).

¹⁷A. Liebsch, Phys. Rev. B **13**, 544 (1976).

¹⁸J. B. Pendry, J. Phys. C **8**, 2413 (1975).

¹⁹D. Liebowitz, M. Sagurton, J. Colbert, and N. J. Shevchik, Phys. Rev. Lett. **39**, 1625 (1977).

²⁰D. Liebowitz and N. J. Shevchik, Phys. Rev. B **18**, 1629 (1978) (following paper).

²¹This follows from evaluation of the commutator $[p, H]$ in terms of eigenstates of the one-electron Hamiltonian.

²²P. J. Feibelman, Surf. Sci. **46**, 558 (1974).

²³K. L. Kliewer, Phys. Rev. Lett. **33**, 900 (1974).

²⁴B. Feuerbacher and R. F. Willis, J. Phys. C **8**, 169 (1976).

²⁵J. Stöhr, G. Apai, P. S. Wehner and F. R. McFeely, R. S. Williams, and D. A. Shirley, Phys. Rev. B **14**, 5144 (1976).

²⁶W. A. Harrison, *Pseudopotentials in the Theory of Metals* (Benjamin, New York, 1966).

²⁷W. F. Krolkowski and W. E. Spicer, Phys. Rev. **185**, 882 (1969).

²⁸E. U. Condon and G. H. Shortley, *Theory of Atomic Spectra* (Cambridge University, Cambridge, England, 1970).

²⁹U. Fano and J. W. Cooper, Rev. Mod. Phys. **40**, 441 (1968).

³⁰I. Lindau, P. Pianetta, K. Y. Yu, and W. E. Spicer, Phys. Rev. B **13**, 492 (1976).

³¹D. E. Eastman and J. K. Cashion, Phys. Rev. Lett. **24**, 310 (1970).

³²N. J. Shevchik, Phys. Rev. B **13**, 4217 (1976).

³³N. V. Smith, M. M. Tramm, J. A. Knapp, J. Anderson, and G. J. Lapeyre, Phys. Rev. B **13**, 4462 (1976).

³⁴P. Heimann, H. Neddermeyer, and H. F. Roloff, Phys. Rev. Lett. 37, 775 (1976).

³⁵T. P. Grandke, L. Ley, and M. Cardona, Phys. Rev. Lett. 38, 1033 (1977).

³⁶B. Feuerbacher and N. E. Christensen, Phys. Rev. B 10, 2373 (1974).

³⁷P. M. Morse and H. Feshbach, *Methods of Theoretical Physics* (McGraw-Hill, New York, 1953), p. 1071.